Dyes and Pigments 111 (2014) 145–155

Contents lists available at ScienceDirect

Dyes and Pigments

journal homepage: www.elsevier.com/locate/dyepig

Short-conjugated zwitterionic cyanopyridinium chromophores: Synthesis, crystal structure, and linear/nonlinear optical properties

Wen Hui Hao [a, b], Pengfei Yan [a], Guangming Li [a], Zhi Yuan Wang [b, c, *]

[a] Key Laboratory of Functional Inorganic Material Chemistry (MOE), School of Chemistry and Materials Science, Heilongjiang University, Harbin 150080, PR China
[b] Department of Chemistry, Carleton University, 1125 Colonel By Drive, Ottawa, Ontario K1S5B6, Canada
[c] State Key Laboratory of Polymer Physics and Chemistry, Changchun Institute of Applied Chemistry, Chinese Academy of Sciences, Changchun 130022, PR China

ARTICLE INFO

Article history:
Received 8 March 2014
Received in revised form
2 June 2014
Accepted 3 June 2014
Available online 14 June 2014

Keywords:
Zwitterionic chromophores
Hyperpolarizability
Solvatochromism
Nonlinear optical
Electro-optic
Fluorescence

ABSTRACT

A new class of short-conjugated zwitterionic cyanopyridinium chromophores with the absorption maxima less than 550 nm were designed and synthesized. These chromophores display a good solubility in organic solvents and exist in a charge-separated ground state, as confirmed by IR, X-ray crystallography, negative solvatochromism and fluorescence studies. They can be doped up to 10% by weight into poly(ether sulfone) and attached onto a methacrylate polymer by grafting. Without optimization of the poling conditions, a high electro-optic coefficient can be readily achieved using the chromophore-grafted nonlinear optical polymers.

1. Introduction

Cyanopyridinium-based zwitterionic chromophores are an important type of the intramolecular charge-transfer (ICT) molecules, in which negatively charged cyano-moiety and pyridium cation are separated by a π-conjugated system. Many interesting characteristics, such as highly charge-separated ground state ($D^{\delta+}-\pi-A^{\delta-}$; D: donor; A: acceptor; δ: degree of CT), large molar extinction coefficient, large negative solvatochromism, large dipole moment (μ), and large negative first molecular hyperpolarizability (β), arise from this peculiar structure, which leads to a wide variety of applications including functional dyes [1], nonlinear optical chromophores [2,3], photochromic materials [4] and chemosensors [5]. Based on the high absorptive feature, various forms of deep-colored solutions, as well as films containing zwitterionic cyanopyridinium chromophore can be obtained [6]. Recently, the cyano moiety of the zwitterionic chromophores was found to be capable of selectively and reversibly coordinating with certain metal ions, resulting in distinct color change due to the switch on/off of CT band [5].

Of course, the most widely studied properties are their large negative first molecular hyperpolarizability (β) and the corresponding figure of merit ($\mu\beta$), which is used to characterize their microscopic nonlinear optical (NLO) efficiencies. Zwitterionic cyanopyridinium chromophores have been demonstrated to be one of the promising classes of second-order NLO materials for electro-optic (EO) applications [7,8]. To fabricate EO devices, NLO chromophores are usually doped into or covalently bonded onto polymers, followed by poling films under an externally applied electric field at the glass transition temperature (T_g) in order to achieve a noncentrosymmetric arrangement with a large macroscopic EO coefficient [9–15]. More recently, a novel approach has been explored in which zwitterionic chromophores with negative β were linked to the neutral-ground-state NLO chromophores with positive β [16–18] and showed the interesting application of zwitterionic chromophores in EO devices.

The previously studied zwitterionic cyanopyridinium chromophores are typically synthesized through the addition between tertiary amines and 7,7,8,8-tetracyanoquino-dimethane (TCNQ), such as DEMI [19], PQDM [20–22] and PeQDM [23] (Fig. 1). Besides complicated procedures and low yield, the chromophores obtained by this method have their absorption maxima limited in the red region of the visible spectrum, usually 600 nm–750 nm.

* Corresponding author. Department of Chemistry, Carleton University, 1125 Colonel By Drive, Ottawa, Ontario K1S5B6, Canada.
E-mail address: wayne_wang@carleton.ca (Z.Y. Wang).

http://dx.doi.org/10.1016/j.dyepig.2014.06.005
0143-7208/

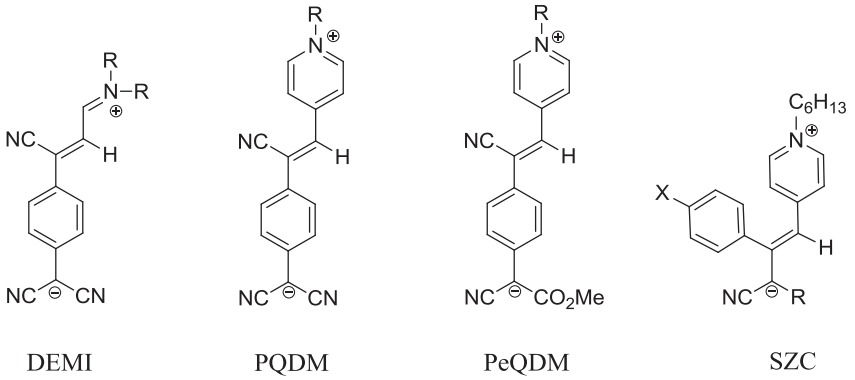

Fig. 1. Chemical structures of zwitterionic chromophores of DEMI, PQDM, PeQDM and **SZC**.

As functional dyes and chromic materials, zwitterionic cyanopyridinium chromophores with a wide absorptive band are desirable (e.g. 400–600 nm). In addition, as a material for NLO application, in order to minimize the optical loss and light damage, the chromophores should ideally be transparent at the communication wavelengths (1310–1550 nm) and have low absorption at visible region, especially near the double frequency wavelengths (650–750 nm). The basic requirement in zwitterionic cyanopyridinium chromophore design calls for the maximal absorption peak to be significantly blue shifted or ideally less than 600 nm [24,25].

Furthermore, zwitterionic chromophores often display poor solubility in normal organic solvents and low compatibility with a polymer matrix. The large dipole moment and planar structure cause the chromophores to aggregate aggressively in the matrix, thereby limiting their loading level in the guest–host polymer systems. The highly polar zwitterionic nature of the chromophores also leads to an anti-parallel dipole arrangement, which could further diminish or even eliminate the macroscopic nonlinearity in bulk and hamper their EO application [19–23].

Therefore, it is desirable to develop a simple versatile method for the synthesis of processable dipolar zwitterionic chromophores with a short transparency cut-off wavelength. To achieve the blue-shifted zwitterionic chromophores, adjusting the conjugation length of the π-electron bridge is important; meanwhile, due to the fact that zwitterionic chromophores often exist as the combination of two limiting resonance forms (zwitterionic and neutral forms), maintaining the zwitterionic structure as the predominant ground state is critical in order to obtain large $\mu\beta$ values [26,27].

Here we report the highly efficient and facile synthesis of a new class of cyanopyridinium chromophores, composed of a pyridium donor and cyano-moiety acceptor (**SZC**, in Fig. 1) and corresponding polymers. These chromophores are purposely designed to have a short conjugation length in order to achieve a blue-shift in absorption. They also have various bulky substituents in order to minimize chromophore dipole–dipole interactions and to improve solubility and compatibility with polymer matrix. The new class of zwitterionic chromophores and polymers are fully characterized by spectroscopic methods, X-ray crystallographic analysis, thermal analysis and nonlinear optical measurement.

2. Experimental section

2.1. Materials

4-Bromophenyl acetonitrile, 4-pyridinecarboxaldehyde, 1,8-diazabicyclo[5.4.0]undec-7-ene (DBU), 1-bromohexane, malononitrile, fluorophenyl acetonitrile, methyl cyanoacetate, cyanoacetic acid, hydroxyethyl cyanoacetate and poly(methyl methacrylate) (PMMA) were purchased from Aldrich Chemicals. Azobisisobutyronitrile (AIBN) was purchased from Aldrich Chemicals and recrystallized from methanol. DMF and DMAc were dried over CaH_2 and distilled under vacuum. Poly(ether sulfone) (PES, commercial trade name: Ultrason E, $T_g = 225\ ^\circ C$) was obtained from BASF. The $LiNbO_3$ wafer was purchased from Thorlabs Inc. (New Jersey, USA) and used for calibration of electro-optic measurement.

2.2. Instruments

^1H and ^{13}C NMR spectra were recorded on a Varian 300 MHz (300 and 75 MHz for ^1H and ^{13}C NMR, respectively) or a Bruker AMX 400 MHz spectrometer using tetramethylsilane (TMS; $\delta = 0$ ppm) as an internal standard. The Fourier transform infrared (FTIR) spectra were recorded on a Perkin–Elmer 1600 or a Bomen Michelson 120 FTIR spectrometer in the regions of 4000–400 cm^{-1}. Mass spectra were measured with a Micromass Quattro LC ESI mass spectrometer (EI and TOF-ESI). The melting points were determined using a Fisher-Johns melting point apparatus. Differential scanning calorimetric analysis was carried out in nitrogen on a TA DSC Q100 with a heating rate of 10 °C/min. Thermogravimetric analysis (TGA) was performed under a nitrogen atmosphere on a Hi-Res TGA 2950 thermogravimetric analyzer with a heating rate of 10 °C/min. The decomposition temperatures (T_d) were determined by 5% weight loss from TGA under nitrogen atmosphere. The UV–Vis–NIR spectra were recorded on a Perkin–Elmer Lambda 900 UV–Vis–NIR spectrometer at room temperature. Fluorescence emission spectra were measured on a PTI fluorescence system. The absorption and fluorescence emission spectra of all the samples were taken in a quartz cuvette with a path length of 10.0 mm. Refractive indices were measured using a Metricon 2010 prism coupler. An alpha-step 200 surface profiler was used for measuring the thin film thickness. The M_w and M_n of the polymers were evaluated in DMF with a Waters GPC system (2414 Refractive Index Detector) with Styragel HR4E and HR5E columns using polystyrene standards.

2.3. Synthesis

2.3.1. Synthesis of 2-(4-bromophenyl)-3-pyridine-4-yl-acrylonitrile (*1*)

Under anhydrous and oxygen-free conditions, to a 250-mL round-bottomed flask, 4-bromophenyl acetonitrile (5.90 g, 30.0 mmol), 4-pyridinecarboxaldehyde (3.0 mL, 30.0 mmol), dry THF (80 mL) and DBU (1 mL) were added. The mixture was heated under reflux for 18 h and then cooled to room temperature. The solvent was removed under reduced pressure; the red residue was

washed with methanol (30 mL), filtered and dried. The final product was an off-white crystalline (3.90 g, 95% yield); mp: 138–140 °C; ^{1}H NMR (300 MHz, DMSO-d_6): δ 8.77 (2H, d, J = 6.0 Hz), 8.15 (1H, s), 7.81 (2H, d, J = 5.9 Hz), 7.76 (4H, m); IR (KBr, cm^{-1}): 2217 (C≡N), 1645 (C=N), 1594, 1588 (C=C); UV–Vis: λ_{max} = 312 nm (DMF); MS (EI, m/z): 284 [M$^+$], 286 [M+2]$^+$.

2.3.2. Synthesis of 2-(4-bromophenyl)-3-N-(n-hexylpyridinium)-4-yl-acrylonitrile bromide salt (**2**)

A mixture of compound **1** (0.350 g, 1.23 mmol), 1-bromohexane (2.8 mL, 20.0 mmol) and benzonitrile (2 mL) was heated under reflux for 18 h. The reaction mixture was cooled and the precipitate was filtered. The crude product was dissolved in hot acetonitrile (10 mL) and then added into hot ether (50 mL). The precipitate was filtered and dried in air to give yellow amorphous powders (0.30 g, 66% yield); ^{1}H NMR (300 MHz, DMSO-d_6): δ 9.22 (2H, d, J = 8.4 Hz), 8.48 (2H, d, J = 8.4 Hz), 8.44 (1H, s), 7.86 (4H, m), 4.64 (2H, t, J = 7.3 Hz), 1.95 (2H, m), 1.32 (6H, m), 0.89 (3H, t, J = 6.9 Hz); IR (KBr, cm^{-1}): 2219 (C≡N), 1637 (C=N), 1604, 1583 (C=C); MS (ESI, acetonitrile, m/z): 369 [M$^+$, 100%]; UV–Vis: λ_{max} = 347 nm (DMF).

2.3.3. Synthesis of 2-(4-fluorophenyl)-3-pyridine-4-yl-acrylonitrile (**3**)

Under anhydrous and oxygen-free conditions, to a 250-mL, round-bottomed flask, 4-fluorophenyl acetonitrile (4.05 g, 30.0 mmol), 4-pyridinecarboxaldehyde (3.20 g, 30.0 mmol), dry THF (90 mL) and DBU (1 mL) were added. The mixture was heated under reflux for 18 h and then cooled to room temperature. The solvent was removed under reduced pressure and the red residue was washed with methanol (30 mL), filtered and dried. The final product was an off-white crystalline (3.40 g, 55% yield). mp: 166–167 °C; ^{1}H NMR (400 MHz, DMSO-d_6): δ 8.75 (2H, d, J = 6.0 Hz), 8.15 (1H, s), 7.80 (2H, d, J = 5.9 Hz), 7.76 (4H, m); IR (KBr, cm^{-1}): 2216 (C≡N), 1592, 1543 (C=C); MS (EI, m/z): 224 [M$^+$, 100%]; UV–Vis: λ_{max} = 319 nm (DMF).

2.3.4. Synthesis of 2-(4-fluorophenyl)-3-N-(n-hexylpyridinium)-4-yl-acrylonitrile bromide salt (**4**)

A mixture of compound **3** (1.75 g, 7.80 mmol), 1-bromohexane (20.0 mL, 143.0 mmol) and benzonitrile (3 mL) was heated under reflux for 18 h. The reaction mixture was cooled to room temperature and the resulting precipitate was filtered. The crude product was dissolved in hot acetonitrile (40 mL) and then poured into ether (250 mL). The precipitate was filtered as yellow amorphous powders (2.40 g, 80% yield). ^{1}H NMR (300 MHz, DMSO-d_6): δ 9.23 (2H, d, J = 8.4 Hz), 8.49 (2H, d, J = 8.4 Hz), 8.45 (1H, s), 7.87 (4H, m), 4.64 (2H, t, J = 7.3 Hz), 1.95 (2H, m), 1.32 (6H, m), 0.88 (3H, t, J = 6.9 Hz); IR (KBr, cm^{-1}): 2224 (C≡N), 1637 (C=N), 1597, 1557 (C=C); MS (ESI, acetonitrile, m/z): 309 [M$^+$, 100%]; UV–Vis: λ_{max} = 341 nm (DMF).

2.3.5. Synthesis of 2-hydroxyethyl cyanoacetate

A mixture of cyanoacetic acid (4.25 g, 50.0 mmol), ethylene glycol (3.41 g, 55.0 mmol), and TsOH (0.2 g) in benzene (15 mL) in a round-bottomed flask equipped with a Dean–Stark trap was heated under reflux. After the calculated volume of water (0.9 mL) was distilled off, the solvent was evaporated and the residue was vacuum distilled to give the product (2.58 g, 40% yield). ^{1}H NMR (300 MHz, DMSO-d_6): δ 3.52 (2H, s), 4.02 (2H, m), 4.40 (1H, s), 4.55 (2H, m); IR (NaCl, cm^{-1}): 3426 (OH), 2268 (C≡N), 1743 (C=O), 1194.

2.3.6. General synthesis of **SZC** chromophores (with **SZC-1** as an example)

Under anhydrous and oxygen-free conditions, to a 50-mL round-bottomed flask, malononitrile (0.50 g, 7.4 mmol), sodium hydride (0.30 g, 60%, 7.5 mmol), compound **4** (1.0 g, 2.6 mmol) and THF (20 mL) were added. After reaction for 30 min at 0 °C, the resulting insoluble inorganic salt was removed by filtration. The filtrate was concentrated under reduced pressure. The residue was purified with the use of column chromatography on silica gel (acetone and hexane, 1:1 v/v). The final product was obtained as orange-red crystal (0.56 g, 63% yield); mp: 167 °C; ^{1}H NMR (400 MHz, DMSO-d_6): δ 7.81 (2H, d, J = 7.1 Hz), 7.36 (2H, d, J = 8.7 Hz), 7.32 (2H, d, J = 8.7 Hz), 6.34 (2H, d, J = 7.1 Hz), 5.88 (1H, s), 3.92 (2H, t, J = 7.4 Hz), 1.63 (2H, t, J = 6.8 Hz), 1.22 (6H, m), 0.83 (3H, t, J = 6.8 Hz); ^{13}C NMR (100 MHz, DMSO-d_6): 161.2, 151.4, 139.8, 133.7, 130.0, 129.9, 119.8, 119.2, 118.2, 116.6, 116.4, 101.7, 56.7, 30.4, 29.8, 24.9, 21.8, 13.7; IR (KBr, cm^{-1}): 2192 ($\upsilon_{C\equiv N}$ of cyano groups), 1640 ($\upsilon_{C=N}$ of picolinium moiety), 1571, 1450; MS (MALTI-TOF, DMF/acetonitrile 1:1): calcd for ($C_{22}H_{22}FN_3$): m/z [M]$^+$: 347.1798; found: m/z 347.1793; UV–Vis: λ_{max} = 486 nm (DMF); T_d = 312 °C; Fluorescence emission: 534 nm (excitation at 486 nm). Anal. Calcd (%) for $C_{22}H_{22}N_3F$: C, 76.06; H, 6.38; N, 12.09. Found: C, 75.93; H, 6.44; N, 12.12.

2.3.7. Synthesis of **SZC-2**

Methyl cyanoacetate (0.74 g, 7.5 mmol) was used; 0.60 g of product (61% yield) was obtained as orange-red crystal. mp: 204–206 °C; ^{1}H NMR (400 MHz, DMSO-d_6): δ 7.72 (2H, d, J = 6.8 Hz), 7.29 (2H, d, J = 8.5 Hz), 7.21 (2H, d, J = 8.5 Hz), 7.20 (1H, s), 6.16 (2H, d, J = 6.8 Hz), 3.88 (2H, t, J = 7.2 Hz), 3.57 (3H, s), 1.63 (2H, t, J = 6.8 Hz), 1.21 (6H, m), 0.83 (3H, t, J = 6.8 Hz); ^{13}C NMR (100 MHz, DMSO-d_6): 163.2, 160.7, 152.2, 139.3, 136.7, 129.9, 122.2, 118.6, 116.3, 116.1, 104.7, 75.1, 56.5, 49.9, 30.4, 29.8, 24.9, 21.7, 13.7; IR (KBr, cm^{-1}): 2180 (C≡N), 1750 (C=O), 1639, 1505; MS (MALTI-TOF, acetonitrile): calcd for ($C_{23}H_{25}FN_2O_2$): m/z [M]$^+$: 380.1900; found: m/z 380.1880. Anal. Calcd (%) for $C_{23}H_{25}N_2O_2F$: C, 72.61; H, 6.62; N, 7.36. Found: C, 72.35; H, 6.51; N, 7.35.

2.3.8. Synthesis of **SZC-3**

2-Hydroxyethyl cyanoacetate (0.99 g, 7.7 mmol) was used; 0.42 g of product (40% yield) was obtained. ^{1}H NMR (400 MHz, DMSO-d_6): δ 9.01 (2H, d, J = 6.8 Hz), 8.12 (2H, d, J = 6.8 Hz), 7.38 (2H, d, J = 8.8 Hz), 7.17 (2H, d, J = 8.8 Hz), 6.92 (1H, s), 4.62 (2H, t, J = 7.6 Hz), 4.48 (2H, t, J = 5.6 Hz), 3.75 (2H, t, J = 5.6 Hz), 1.93 (2H, t, J = 6.8 Hz), 1.28 (6H, m), 0.86 (3H, t, J = 6.8 Hz); IR (KBr, cm^{-1}): 3387 (OH), 2934, 2175 (C≡N), 1637 (C=O), 1509; MS (EI, m/z): 410 [M$^+$, 100%]; UV–Vis: λ_{max} = 496 nm (DMF), λ_{max} = 556 nm ($CHCl_3$).

2.3.9. Synthesis of **SZC-4**

Under anhydrous and oxygen-free conditions, to a 25-mL round-bottomed flask, malononitrile (0.027 g, 0.40 mmol), sodium hydride (0.024 g, 60%, 0.60 mmol) and compound **2** (0.10 g, 0.2 mmol) were added. After reaction for 30 min at 0 °C, the resulting insoluble inorganic salt was removed by filtration. The filtrate was concentrated under reduced pressure. The residue was purified with the use of column chromatography on silica gel (acetone and hexane, 1:1 v/v) to give the final product as orange-red crystal (0.059 g, 65% yield). mp: 196 °C; ^{1}H NMR (400 MHz, DMSO-d_6): δ 7.81 (2H, d, J = 7.1 Hz), 7.36 (2H, d, J = 8.7 Hz), 7.32 (2H, d, J = 8.7 Hz), 6.34 (2H, d, J = 7.1 Hz), 5.88 (1H, s), 3.92 (2H, t, J = 7.4 Hz), 1.63 (2H, t, J = 6.8 Hz), 1.22 (6H, m), 0.83 (3H, t, J = 6.8 Hz); IR (KBr, cm^{-1}): 2190 ($\upsilon_{C\equiv N}$ of cyano groups), 1640 ($\upsilon_{C=N}$ of picolinium moiety), 1571, 1450 ($\upsilon_{C=C}$ aromatic ring); MS (EI, m/z): 407 [M]$^+$, 409 [M+2]$^+$; UV–Vis: λ_{max} = 486 nm (DMF); T_d = 323 °C (TGA).

*2.3.10. Synthesis of **SZC-5***

A Schlenk flask was charged with THF (23 mL), methacryloyl chloride (0.53 mL, 5.4 mmol), **SZC-3** (1.86 g, 4.0 mmol) and Et_3N (0.76 mL, 5.4 mmol). The reaction mixture was stirred at ambient temperature for 6 h and then diluted with 200 mL of ether (200 mL). The organic layer was washed with water (2 × 200 mL) and brine (200 mL) and then dried over anhydrous K_2CO_3. The solvent was removed under reduced pressure, and the crude product was purified by chromatography on an alumina column, eluting with dichloromethane. The red band was collected to give **SZC-5** as red powder (1.52 g, 70% yield). ^{1}H NMR (400 MHz, DMSO-d_6): δ 8.99 (2H, d, J = 6.8 Hz), 8.07 (2H, d, J = 6.8 Hz), 7.37 (2H, d, J = 8.8 Hz), 7.14 (2H, d, J = 8.8 Hz), 6.91 (1H, s), 5.67 (1H, t, J = 1.6 Hz), 5.60 (1H, t, J = 1.6 Hz), 4.61 (2H, t, J = 7.2 Hz), 4.47 (2H, t, J = 6.2 Hz), 4.07 (2H, t, J = 6.2 Hz), 1.98 (3H, s), 1.92 (2H, t, J = 6.8 Hz), 1.23 (6H, m), 0.83 (3H, t, J = 6.8 Hz); IR (KBr, cm^{-1}): 2177 (C≡N), 1739 (C═O), 1672 (C═C), 1637 (C═O).

*2.3.11. A typical procedure for the synthesis of polymer **NP***

A two-neck, round-bottomed flask was charged with **SZC-5** (0.105 g, 0.220 mmol), methyl methacrylate (0.450 mL, 4.18 mmol), AIBN (3.0 mg) and of dry benzene (1 mL). The reaction mixture was heated to 80 °C under nitrogen for 18 h. After dilution with benzene, the polymer was precipitated into methanol and collected as light red amorphous powder on filter (0.11 g, 89% yield). ^{1}H NMR ($CDCl_3$): δ 8.5, 8.2, 7.5, 7.0, 4.3, 3.6, 1.3–1.5, 0.8–1.1; IR (KBr, cm^{-1}): 2177 (C≡N), 1756 (C═O), 1731 (C═O), 1637, 1485, 1150; UV–Vis: λ_{max} = 502 nm (DMF), 558 nm ($CHCl_3$). **NP-2** (Number-average molecular weight (M_n) of 51,954 Da, polydispersity index (PDI) of 1.25): T_g = 126 °C, T_d = 232 °C.

2.4. Single crystal X-ray diffraction

All diffraction measurements were carried out on a Bruker SMART APEX CCD diffractometer with graphite-monochromated Mo-Kα (λ = 0.71073 Å) radiation. Data were collected using the Bruker SMART detector, processed using the SAINT Plus package from Bruker. The structures were solved by direct methods (SHELXS-97) and expanded using Fourier techniques (SHELXL-97). All calculations were performed using the Bruker SHELXTL97 crystallographic software package.

2.5. Quantum yield measurement

The fluorescence emission spectra were measured with a PTI spectrofluorometer. The fluorescence emission spectra of **SZC** (2 × 10^{-5} M) were measured at 25 °C, with excitation at 470 nm. The fluorescent quantum yield (Φ_F) of **SZC** were obtained with reference to Rhodamine 6G (Φ_F = 0.88 in ethanol) [28]. The quantum yield (Φ) of **SZC** is expressed by eq. (1) [29], where the subscript "r" stands for the reference and "x" for the sample), A is the absorbance at the excitation wavelength, I (λ) is the relative intensity of the exciting light at wavelength λ, n is the refractive index of the solvent for the luminescence, and D is the area (on an energy scale) of the luminescence spectra. The samples and the reference were excited at the same wavelength. The sample absorbance at the excitation wavelength was kept as low as possible to avoid fluorescence errors (A_{exc} <0.1).

$$Q_x = Q_r\left(\frac{A_r(\lambda_r)}{A_x(\lambda_x)}\right)\left(\frac{I(\lambda_r)}{I(\lambda_x)}\right)\left(\frac{n_x^2}{n_r^2}\right)\left(\frac{D_x}{D_r}\right) \quad (1)$$

2.6. Thin film preparation and EO coefficient measurement

Doping **SZC** into PES to form a host–guest system was done with 5 wt% chromophore content. To cast films, a DMF solution (2 wt%) containing a chromophore and host polymer or a chromophore-grafted polymer such as **NP** polymers was stirred overnight at room temperature in darkness. The solution was filtered through a 0.2-μm syringe filter and casted onto ITO glass to form the films of about 1–3 μm thickness and then baked at 45 °C overnight under nitrogen. The films were further heated in a vacuum oven overnight at 85 °C. Then a layer of gold with a thickness of 100–150 nm was sputtered or vacuum deposited on the films as the top electrode for electric poling. During the thermo-electric poling process, the sample cells were gradually heated to the final poling temperature, while the voltage was gradually applied across the polymer films with an average of 70 V/μm. The EO coefficients of the poled samples were measured at the laser wavelength of 1550 nm using the Teng-Man reflection technique setup [30]. The EO measurement was calibrated using a commercial $LiNbO_3$ wafer (r_{33} = 31 pm/V at 1550 nm).

3. Results and discussion

*3.1. Preparation of the **SZC** chromophores*

The general synthesis of **SZC** chromophores is shown in Scheme 1. In order to introduce the alkene bridge and functional bulky groups in the center of the chromophores, 4-fluorophenyl acetonitrile (or 4-bromophenyl acetonitrile) and 4-pyridinecarboxaldehyde were used as starting materials to prepare compound **1**. The crucial pyridinium salt **2** was then prepared by alkylation of compound **1** with 1-bromohexane in benzonitrile. The alkylated pyridinium is highly reactive towards active methylene compounds, such as malononitrile, cyanoacetates, allowing for a highly efficient nucleophile-replacement of the cyano group in the central part of compound **1** and clean access to **SZC** chromophores under mild conditions without any catalysts. The target chromophores including a bromo-cyanide containing chromophore (**SZC-4**) and three fluoro-cyanide containing chromophores were prepared in good yields (>60%). Amongst **SZC** chromophores, hydroxyl-containing chromophore (**SZC-3**) is considered to be a potential monomer for the synthesis of grafted NLO polymers. Halides (e.g., F or Br) on the aromatic rings may alter the polarity of the chromophores and also allow for further functionalization on the phenyl rings, for example, by the Suzuki cross-coupling reaction. The long aliphatic chains on the nitrogen of pyridine are deemed to impart the solubility to the chromophores. To prepare **SZC-3**, the required 2-hydroxyethyl cyanoacetate was synthesized according to a known procedure [31].

The **SZC** chromophores were fully characterized by ^{1}H NMR, ^{13}C NMR, IR and mass spectrometry. In the IR spectrum of **SZC-1** (Fig. S5), the cyano group is observed at 2192 cm^{-1}, and the intensity of the peak is strikingly high, which is characteristic of the cyano group connected to an electron-rich group with a negative charge. In order to illustrate the extent of ground-state charge separation, some IR data of compounds **1** and **2**, **SZC-1**, **SZC-2** and other model compounds are listed in Table 1. Since the stretching frequency of the cyano groups is sensitive to the vicinal electron density, it is a good probe for the ground-state charge transfer. The bond strength and therefore the vibrational frequency of CN groups are reduced by the presence of increased vicinal electron density, which interacts with the π^* orbital of the CN group [32].

The stretching frequency of ν_{CN} was found at 2178 cm^{-1} for lithium dicyano-phenylmethanide ($Li^+[C(CN)_2Ph]^-$), which indicates a full formal vicinal negative charge, while the stretching

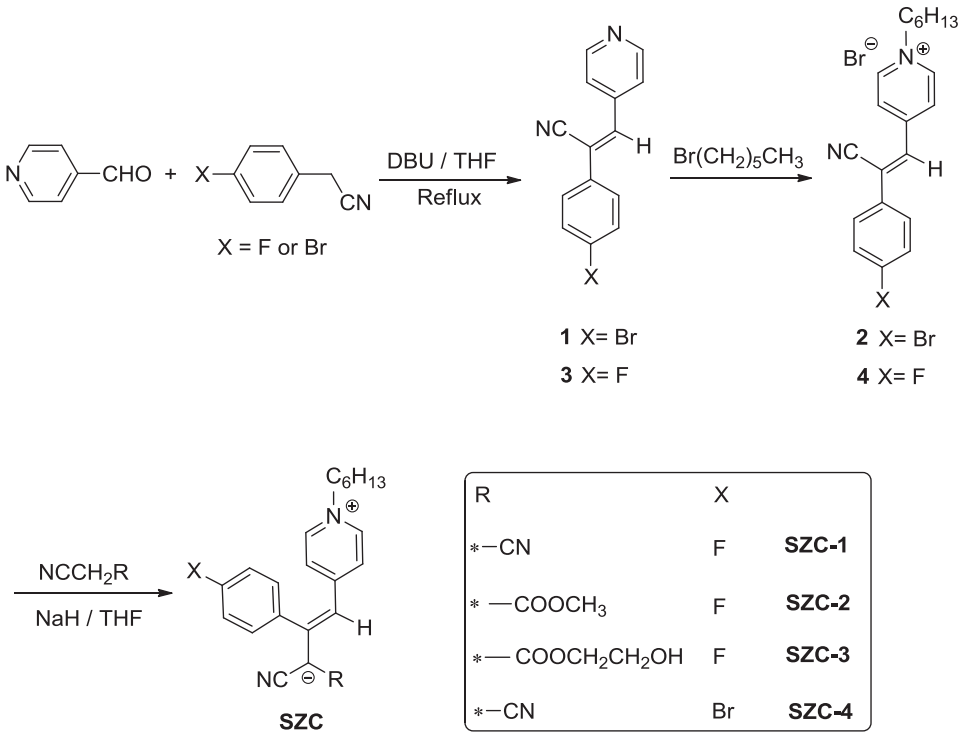

Scheme 1. Synthesis of zwitterionic chromophores **SZC**.

frequency, $\nu_{CN} = 2226\ cm^{-1}$, for TCNQ serves as a model without formal vicinal charge [33]. The CN stretches at 2220 cm^{-1} and 2224 cm^{-1} for intermediate compounds **1** and **2**, respectively, are from typical neutral conjugated cyano groups. On the other hand, the lower values for **SZC-1** (2192 cm^{-1}) and **SZC-2** (2180 cm^{-1}) imply considerable CT character in the ground state. In comparison, the smaller $\nu_{C\equiv N}$ frequency of PeQDM (2146 cm^{-1}) with that of PQDM (2173 cm^{-1}) indicate that PeQDM with one cyano and one ester group at the acceptor part gain more aromatization stabilization than PQDM, which shows that PeQDM has a higher molecular hyperpolarizability and larger EO coefficient than PQDM [31]. A similar trend of the smaller $\nu_{C\equiv N}$ frequency for **SZC-2** than **SZC-1** was observed.

3.2. Structure by X-ray crystallography

Further evidence for the formation of zwitterionic chromophores is provided by X-ray crystallography of **SZC-1** (Fig. 2) [34]. Single crystal of **SZC-1** was obtained by slow crystallization from a hexane/acetone solution at room temperature.

The central bond length between C7 and C11 (1.384 Å) is similar to the value observed in other zwitterionic compounds [1], which clearly indicates the double bond π-bridge separating the pyridinium and dicyanomethanide groups. This conclusion is also supported by additional selected bond lengths shown in Table 2.

The bond lengths between C7 and C8 (1.408 Å), C7 and C11 (1.384 Å) suggest electron delocalization among the three carbon atoms. By comparing the observed two C—CN bonds (1.411 Å and 1.420 Å) with the one (1.427 Å) in typical TCNQs, there is a substantial negative charge localization within the $-C(CN)_2$ group; the elongated CN (1.151 Å and 1.147 Å) bond compared to that in typical TCNQs (1.144 Å) [35] indicates a charge resonant stabilization via the two CN groups.

For comparison, the well-known Brooker dye (Scheme 2), which has a similar conjugated backbone and a length of the central bond of 1.35 Å in the solid state, is considered as the prototype of a zwitterionic merocyanine dye, with an estimated degree of the zwitterionic form of 81.8% in its ground state [36]. The longer central bond, 1.384 Å, in **SZC-1** indicated that less than 80% of the zwitterionic form in its ground state. Compared to the central bond

Table 1
Selected IR data for **1**, **2**, **SZC-1** and **SZC-2**.

Compound	ν_{CN} (cm^{-1})	Compound	ν_{CN} (cm^{-1})
$Li^+[C(CN)_2Ph]^-$	2178[33]	**SZC-1**	2192
TCNQ	2226[33]	**SZC-2**	2180
1	2220	**PQDM**	2173[21]
2	2224	**PeQDM**	2146[23]

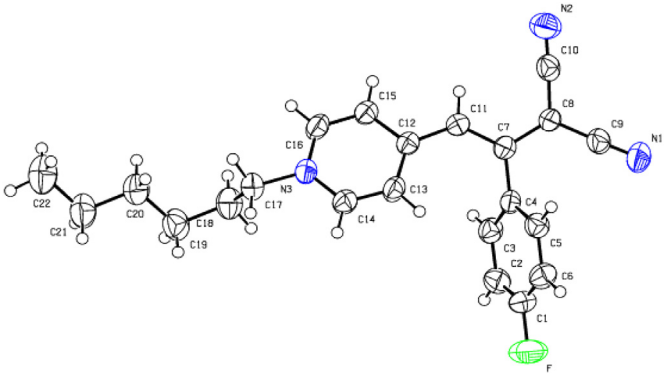

Fig. 2. ORTEP drawing of the structure of **SZC-1** in the crystal with atomic number. Hydrogen atoms were omitted for clarity. The crystal data for **SZC-1** is given as followed: $C_{22}H_{22}FN_3$, $M = 347.43$, monoclinic, $a = 10.485(3)$ Å, $b = 8.809(2)$ Å, $c = 21.313(5)$ Å, $\alpha = 90.00°$, $\beta = 100.628(4)°$, $\gamma = 90.00°$, V = 1934.7(8) $Å^3$, $T = 293$ (2) K, Space group P 2(1)/c, $Z = 4$, 11,920 reflections measured, 4589 independent reflections. The final R values were 0.0505($I > 2$sigma (I)). The final $R1$ values were 0.1084 (all data). The final $wR2$ values were 0.0902 (all data). CCDC number: 861785.

Table 2
Selected bond distances for **SZC-1** in the crystal.[a]

Atom1	Atom2	Å	Atom1	Atom2	Å
C4	C7	1.487(2)	C16	N3	1.352(1)
C7	C11	1.384(4)	C14	N3	1.349(2)
C7	C8	1.408(2)	C17	N3	1.480(1)
C11	C12	1.416(2)	C8	C9	1.411(2)
C12	C13	1.409(2)	C8	C10	1.420(2)
C12	C15	1.413(2)	C9	N1	1.147(2)
C13	C14	1.352(2)	C10	N2	1.151(2)
C15	C16	1.349(2)	C1	F	1.362(4)

[a] Estimated value in parenthesis refer to the last digit.

length of PeQDM (1.354 Å, double bond character), **SZC-1** has a lower degree of charge transfer in ground state than that of PeQDM.

Although the bond lengths in the conjugated bridge and acceptor part clearly demonstrated a zwitterionic molecular structure of **SZC-1**, the bond length of the pyridinium ring is quinoidal rather than aromatic. Similar phenomena have also been reported for other zwitterionic molecules such as DEMI [19] and PeQDM [23]. Therefore, the best description of the ground state structure of such chromophores is the combination of the two limiting forms, zwitterionic and neutral forms wherein the zwitterionic contribution predominates.

As shown in Fig. 3 (left), two **SZC-1** molecules are arranged in an antiparallel fashion with an intermolecular distance of 4.0645 Å between the aromatic backbones in the crystal cell. A smaller slip angle ($\theta = 48.8°$) than that in PeQDM-Ben ($\theta = 64.5°$) is observed which indicated that there is no H-aggregation between two chromophores. The intermolecular distance (d) is considerably larger than the sums of van der Waals radii between planar cofacial π-electron systems (~3.50 Å) [37], the dihedral angle between the pyridinium and benzene rings is 65.65°, result in the difficulty in close face-to-face packing of the aromatic rings in these central bulky molecules. Therefore, incorporation of bulky groups onto the central moiety is an effective strategy to minimize molecular interaction. The weak electrostatic interactions between **SZC-1** (compared to PQDMs and PeQDMs) make these chromophores soluble not only in polar solvents such as DMF, acetonitrile (ACN) and methanol, but also moderately soluble in less polar solvents such as chloroform, tetrahydrofuran (THF) and benzene.

3.3. Solvent-dependent optical property of *SZC* chromophores

All of **SZC** chromophores present a strong CT band in the visible region of the spectrum, the largest absorption wavelengths of **SZC-1** and **SZC-2** in selected solvents are collected in Table 3. **SZC-1** shows good transparency, approximately 200 nm blue-shift of the maximum absorption of **SZC-1** in DMF solution was observed compared with that of PQDM [21]. The CT band of **SZC-1** exhibits negative solvatochromic effect, a hypsochromic shift from THF ($E_T = 37.4$) to MeOH ($E_T = 55.5$) is about 15 nm toward shorter wavelengths with increasing solvent polarity. The negative solvatochromism result indicates that the charge-separated resonance

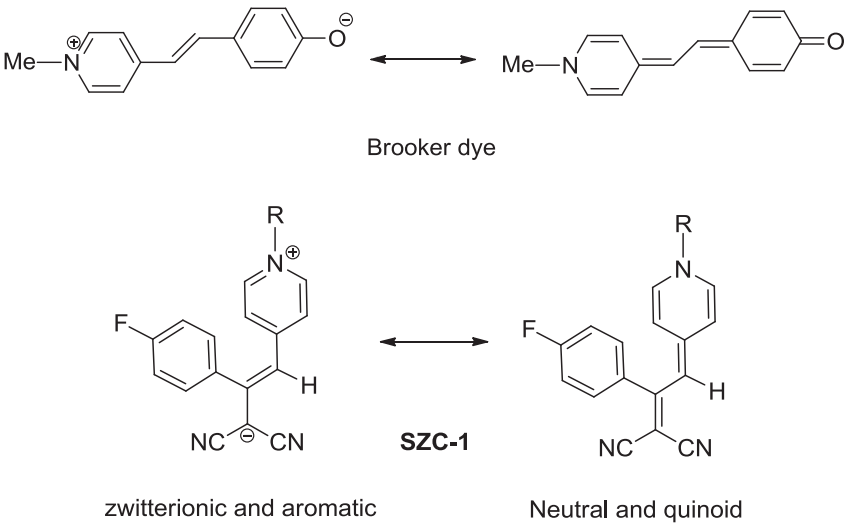

Scheme 2. Resonance structures of Brooker dye and chromophore **SZC**.

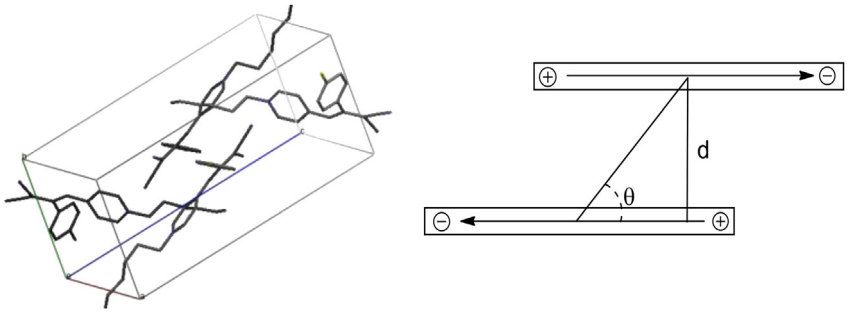

Fig. 3. Crystal packing diagrams of chromophore **SZC-1** (the hydrogen atoms are omitted for clarity) (left); Model for a centrosymmetric dimer of two dipolar dyes, θ is the slip angle of the dimer, d is the distance between the π–π systems (right).

Table 3
λ_{max} of **SZC** chromophores in different solvents.

Compound	THF 7.6[a]/ 37.4[b]	Acetone 20.7/42.2	Methanol 32.7/55.4	DMF 36.7/43.2	ACN 37.5/ 45.6	DMSO 46.7/45.1
SZC-1	495	487	480	485	483	484
SZC-2	502	495	486	493	490	492

[a] Solvent Dielectric Constant (ε) [39].
[b] Reichardt $E_T^{(30)}$ values [38].

form of **SZC-1** is more dominant in the ground state than the excited state ($\mu_g > \mu_e$) [38].

In comparison, the magnitude of the solvatochromic shift in the PQDM chromophores (on average 113 nm) [21] is 7.5 times larger than that in the **SZC** chromophores (on average 15 nm). This can be explained by the magnitude of the gain in resonance stabilization energy upon aromatization of the two donor and acceptor units. The gain in aromaticity for the **SZC** chromophores is expected to be less than that in the case of PQDMs due to the absence of one benzene unit in the conjugated bridge.

As shown in Fig. 4, the strongest emission band of **SZC-1** has a maximum at 530 nm. The fluorescence spectrum of **SZC-1** associated with the lowest excited singlet state displays a mirror image of the corresponding absorption band (485 nm) with a Stokes shift of 45 nm. As shown in Fig. 5, a set of fluorescence spectra of **SZC-1** show a gradual blue shift with increasing solvent polarity, from 539 nm in 1,4-dioxane to 524 nm in methanol. The negative polarity-dependent results are consistent with the negative solvatochromism of **SZC-1**, which further confirms the charge-separated ground state of these chromophores.

In comparison with DEMI and PpQDM [5], the Stokes shift values are dramatically influenced by an increase in the conjugation length from **SZC** to DEMI to PpQDM (Table 4). The large Stokes shift of PpQDM could be explained by the magnitude of the gain in resonance stabilization energy upon aromatization of the donor and acceptor units. The gain in aromaticity for DEMI is expected to be less than that of PpQDMs due to the absence of one aromatic ring in the donor. **SZC** have the shortest conjugation length and accordingly have the smallest Stokes shift among all.

3.4. Dipole moment and molecular hyperpolarizability

The ground-state dipole moment (μ), first hyperpolarizability (β) and the corresponding figure of merit ($\mu\beta$) are representative characteristics of zwitterionic chromophores. Large dipole moments are expected on the basis of the zwitterionic ground state structure of **SZC**. Since the ester is considered to be a weaker electron acceptor than the nitrile, the dipole moment of **SZC-2** is expected lass than **SZC-1**. A decrease in dipole moment from **SZC-1** to **SZC-2** has been confirmed experimentally by the most common method based on dielectric and refractive index measurements according to Debye's theory. The changes in dielectric constant and refractive index of solutions of the chromophores in nonpolar solvents are measured to give a dipole moment of 21.6 D for **SZC-1** and 11.4 D for **SZC-2** (Table 5).

The first hyperpolarizabilities of **SZC** chromophores are measured by hyper-Rayleigh scattering (HRS) method in DMF solution at 1.07 μm wavelength. The β_{zzz} values are -320×10^{-30} esu for **SZC-1** and -495×10^{-30} esu for **SZC-2**, assuming all other components are negligible. More details about the setup, data collection, and dispersion modeling are given in our previous reports [19]. The structural feature of DEMI, PQDM and PeQDM implies that the aromatic/quinoidal bridging unit is critical in maintaining a charge-separated state and might be necessary for their optical nonlinearity. However, this bridging unit is absent in **SZC** chromophores, which still exhibit optical nonlinearity. In addition, either the replacement of the third cyano group on the central part or substitutions on one of the cyano group of the acceptor does not significantly change the dipole and optical nonlinearity of **SZC** chromophores. Further comparison can be made between **SZC** and the adducts of N,N-dimethylaniline/tetracyanoethylene (TCNE) [41], as the former exhibits a negative

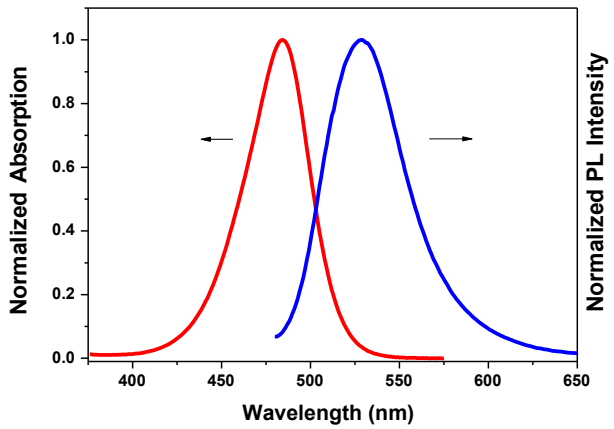

Fig. 4. The normalized absorption and emission spectra of **SZC-1** in DMF (2×10^{-5} M).

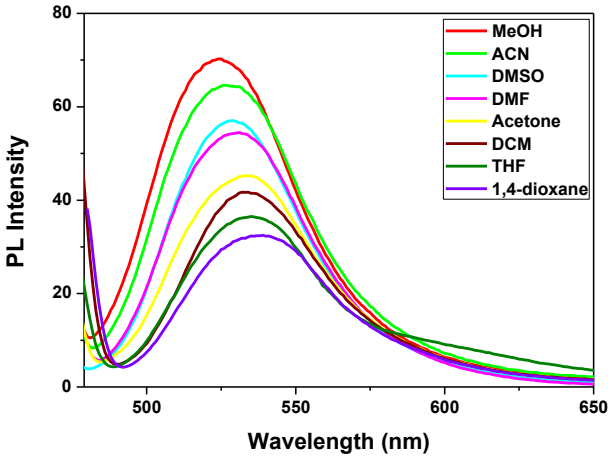

Fig. 5. Fluorescence spectra of **SZC-1** solutions with excitation at 460 nm. The successive maxima correspond to methanol, ACN, DMSO, DMF, acetone, DCM, THF and 1,4-dioxane.

Table 4
Optical properties of **SZC**, DEMI and PpQDM in DMF.

Compound	λ_A (nm)[a]	λ_F (nm)[b]	$\lambda_F - \lambda_A$ (nm)	Φ_F (%)
SZC-1	485	530	45	0.40[c]
SZC-2	493	533	40	0.27[c]
DEMI	690	770	80	–
PpQDM	680	875	195	0.20[d]

[a] Maximal wavelength of absorption and fluorescence measured at a concentration of 2×10^{-5} M in DMF. Excitation wavelength is 470 nm for **SZC-1** and **SZC-2**; 670 nm for DEMI and PpQDM.
[b] Maximal wavelength of absorption and fluorescence measured at a concentration of 2×10^{-5} M in DMF. Excitation wavelength is 470 nm for **SZC-1** and **SZC-2**; 670 nm for DEMI and PpQDM.
[c] Fluorescence quantum yield, relative to Rhodamin 6G ($\Phi_F = 0.88$ in ethanol).
[d] Fluorescence quantum yield measured in DMF, relative to IR-125 ($\Phi_F = 0.13$ in DMSO) [40].

Table 5
Dipole moment and hyperpolarizability of **SZC** and other chromophores.

Chromophore	μ (D)	β[c] (10^{-30} esu)	β_0 (10^{-30} esu)	$\mu\beta$ (10^{-48} esu)
SZC-1	21.6[a]	−320	–	−6720
SZC-2	11.4[a]	−495	–	−5643
PQDM-Met	38[b]	−1865	247–397[d]	−70,870
PeQDM-Ben	40[b]	−1800	416–546[d]	−70,000
DEMI	27[b]	–	350[e]	−9450[f]

[a] Experimental value measured in $CHCl_3$.
[b] Theoretical value (Experimental value has not been measured in chloroform due to solubility difficulties) [7,26].
[c] The experimental value measured by HRS in DMF at 1.07 μm.
[d] Static values derived by means of the single-mode vibronic model (serving as a lower limit); Static values obtained from the purely homogeneous vibronic-like model (serving as an upper limit) [26].
[e] Measured in chloroform [7].
[f] Measured value of $\mu\beta_0$ in chloroform [7].

first molecular hyperpolarizability and the latter in the predominantly non-charge separated ground state shows the positive values.

3.5. Thermal properties

For EO applications, the chromophore is typically doped in a host polymer and then subjected to electric poling at elevated temperatures. Thermal stability of the chromophore is a key parameter for the selection of host polymer and poling temperature. Thermal properties of **SZC** chromophores were evaluated by differential scanning calorimetry (DSC) and thermogravimetric analysis (TGA). Thermogravimetric analysis of **SZC-1** and **SZC-2** was done under nitrogen and the onset temperatures for 5% weight loss were found at 312 °C and 323 °C, respectively (Fig. 6a), being higher than those of PQDM (287 °C) [21] and PeQDMs (215–287 °C) [23]. The characterization by DSC revealed typical phase transitions, namely crystallization at 130 °C and 120 °C and melting process at 167 °C and 196 °C for **SZC-1** and **SZC-4**, respectively (Fig. 6b). During the cooling process, no crystallization was observed for these two chromophores.

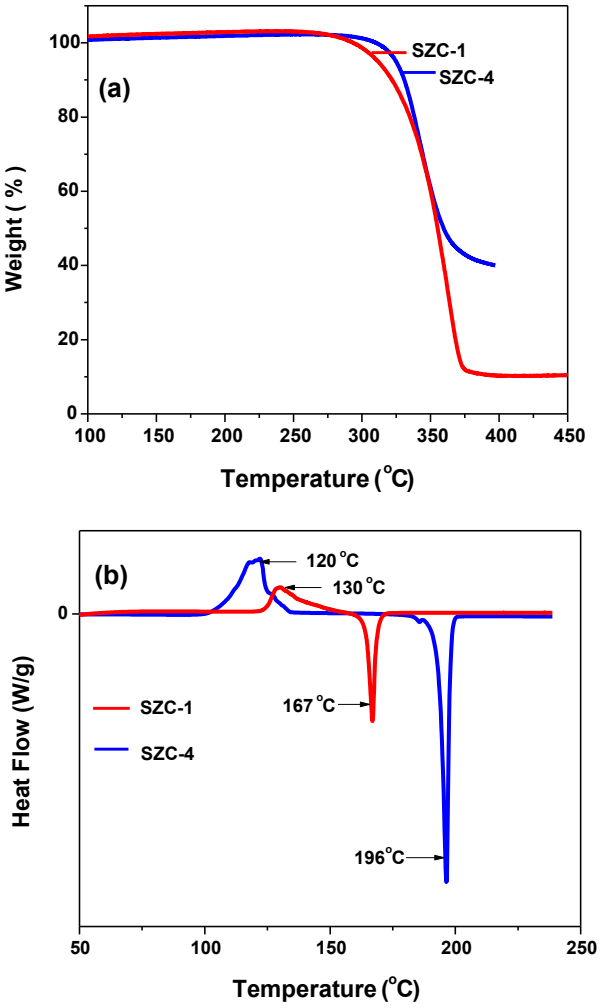

Fig. 6. TGA thermograms (a) and DSC traces (b) of **SZC-1** and **SZC-4**.

3.6. Synthesis of *SZC*-containing NLO polymers (*NP*)

To achieve a large and stable macroscopic EO activity, chromophores are usually doped in a polymer host or covalently bonded onto a polymer and then oriented under an externally applied electric field at the glass transition temperature (T_g) of the materials in order to obtain a noncentrosymmetric order. To choose a suitable host for **SZC**, PMMA and PES are typically good candidates, due to their availability, good processability and suitable compatibility with zwitterionic chromophores [42–44]. A relatively large amount of **SZC-1** (5–10 wt%) could be blended into PMMA and PES, forming the films with no phase separation. Considering a higher T_g, PES was used to make **SZC**/PES guest–host polymers for EO measurement.

To incorporate **SZC** chromophores into polymer by copolymerization, **SZC-5** monomer was needed and thus synthesized by the reaction of **SZC-3** with methacryloyl chloride. The general synthesis of **SZC**-containing NLO polymers (**NP**) by free radical polymerization of **SZC-5** with methyl methacrylate (MMA) is shown in Scheme 3.

The IR spectrum of **SZC-5** displayed the characteristic bands of cyano group at 2177 cm^{-1} and of the esters at 1739 and 1672 cm^{-1}. The maximal absorption of **SZC-5** is at 556 nm in chloroform and 496 nm in DMF, which indicates that **SZC-5** has the same charge-separated ground state as **SZC-3**. Polymers **NP-1** and **NP-2** were obtained in 85–90% yields as light red powders (Table 6). The IR spectra of the **NP** polymers exhibit the characteristic peaks for the cyano groups at 2177 cm^{-1}. The ^1H NMR spectra of two **NP** polymers displayed the expected peaks corresponding to the structures of both MMA and **SZC** chromophore (Fig. S8).

The contents of **SZC** chromophore in **NP** polymers were determined from the UV absorption that is calibrated using **SZC-1** in DMF and found to be 7 wt% and 14 wt% for **NP-1** and **NP-2**, respectively. Negative solvatochromism for **NP** polymers was also confirmed, as the absorption of **NP-1** is at 558 nm in $CHCl_3$ and 502 nm in DMF. **NP** Polymers have good thermal stability (T_d > 232 °C). The T_g value of **NP-2** (126 °C) is higher than that of **NP-1** (95 °C), due to a higher content of polar **SZC** in the polymer. **NP** polymers have good solubility in common organic solvents such as $CHCl_3$, benzene, ACN and DMF. Flexible and transparent films without any phase separation can be readily prepared on ITO coated glass by solution casting and are suitable for electric poling and EO measurement.

3.7. Poling and EO properties

To investigate the potential of **SZC** chromophores in EO applications, both **SZC**/PES doped guest–host polymers and NLO polymers **NP** were poled and the EO coefficients were assessed. For the poling studies, **SZC**/PES films with a thickness of 1–3 μm were

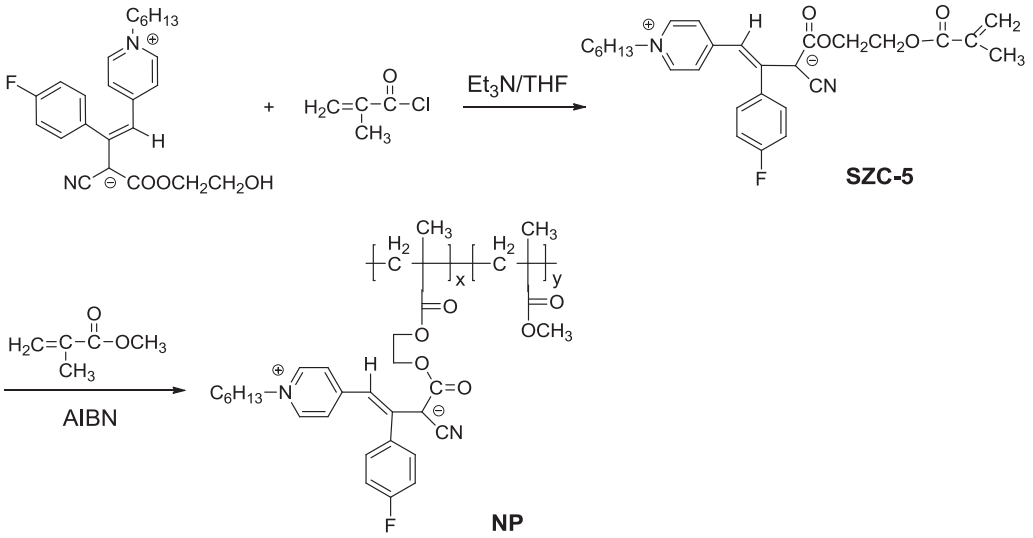

Scheme 3. Synthesis of **SZC**-containing **NP** polymers.

prepared by casting a solution in DMF (2 wt%/V) onto ITO glass substrates. **NP** polymer films with a thickness of 1–3 μm on ITO glass were prepared by solution casting. The films were dried at 60–80 °C under vacuum (1 mmHg) for 24 h before sputtering a thin layer (100–150 nm) of gold as a top electrode onto the polymer films. The parallel-electrode poling was carried out under the protection of nitrogen in dark and the sample cells were gradually heated from room temperature to the poling temperature, about 5–10 °C below the T_g of the polymer films (e.g., 190 °C for **SZC**/PES) at a heating rate of 5 °C/min. The poling field was then applied to the sample at a ramping rate of 10 V/min. During the poling process, the electric current was monitored to optimize poling efficiency and to control local electrical breakdown in the films. After the films were held at the final poling temperature for 20 min, the heating was turned off while keeping the poling field. After reaching room temperature, the poling voltage was taken off and the EO coefficient, r_{33} was determined on a Teng-Man reflection setup immediately at 1550 nm. The EO properties of **SZC**-doped polymers and **NP** polymers were summarized in Table 7.

Although **SZC** chromophores exhibit moderate $\mu\beta$ values but still ten times less than PQDM (Table 5), **SZC** (5%) doped PES films display almost the same EO coefficients as PQDM (1 wt%) doped PES films (21 pm/V) [23]. **SZC** can be doped up to 10 wt% into PES, 5 times higher than PQDM (about 2 wt%), which can be attributed to less dipole–dipole interaction of the short-conjugated **SZC** molecules. In addition, due to relatively smaller dipole moment, **SZC** chromophores (11–20 D) are more compatible with and soluble in PES than PQDM (38–40 D).

The poled **SZC**-doped PES polymers showed a small EO coefficient (<20 pm/V), presumably due to a low number density of **SZC**. Attempt to increase the **SZC** content to above 10 wt% led to the formation of brittle films that are not suitable for poling. To achieve a higher poling efficiency and thus higher EO coefficient, the polymer with high chromophore content is desirable. Thus, **NP** polymers with 7 and 14% **SZC** were subjected to poling. In comparison with **SZC**-doped PES films, **NP** polymer films showed a better stability to the electric field above 70 V/μm and displayed the EO coefficients of 24 and 30 pm/V for **NP-1** and **NP-2** polymers, respectively. A slightly higher EO coefficient for **NP-2** polymer is likely due to its higher chromophore content than **NP-1**. As expected, the EO coefficient (30 pm/V) of the poled **NP-2** (14 wt% chromophore) is higher than that of the **SZC** doped PES system (5 wt%) and is indeed comparable to that of lithium niobate (31 pm/V). It is known that a trade-off between the chromophore content and poling efficiency for highly polar chromophore-polymer systems and a maximum of chromophore incorporation exists for a maximal poling efficiency, depending on the chromophore polarity and dipole–dipole interaction. For PQDM, an amount of 11 wt% can be covalently incorporated in polyimide to achieve a maximum of EO coefficient [6]. A higher concentration of **SZC** (14%) in a poled polymer with the EO coefficient of 30 pm/V can be attributed to the short conjugation length and low dipole–dipole interaction of **SZC**. Further increase of the concentration of **SZC** in a polymer is highly possible when using a more polar polymer as a carrier, which should lead to a higher EO coefficient.

4. Conclusions

Short-conjugated zwitterionic cyanopyridinium chromophores (**SZC**) with a rigid non-planar structure and the absorption less than 550 nm were designed and synthesized by the use of nucleophile substitution reaction between cyano-pyridinium salt and cyanoacetates without any catalysts. The synthetic process developed was simple and versatile and allows the preparation of a blue-shift **SZC** with high yield, the easy introduction of functional groups and the

Table 6
Characterizations of **NP** polymers.

Polymer	X (wt%)	Y (mol%)	λ_{max} (DMF, nm)	T_g (°C)	T_d (°C)
NP-1	7	95	502	95	264
NP-2	14	90	498	126	232

Table 7
EO properties of **SZC**-doped PES and **NP** polymers.

NLO polymer	N (wt%)	Film thickness (μm)	n	Poling temperature (°C)	r_{33} (pm/V)
SZC-1/PES	5	2.12	1.6206	190	20
SZC-2/PES	5	2.06	1.6204	180	18
NP-1	7	2.01	1.4972	90	24
NP-2	14	1.89	1.4970	120	30

N: chromophore content in polymer.
n: refractive index at 1550 nm.

alteration of the geometry of **SZC**. The new zwitterionic cyanopyridinium chromophores display excellent solubility in organic solvents, good film forming ability, higher loading level in polymer matrix and good thermostability. IR, X-ray crystallography, negative solvatochromism and fluorescence studies confirm the charge-separated ground state of **SZC**. Absorption spectra of **SZC** chromophores show a blue shift by nearly 200 nm in comparison with the previously studied PQDM chromophores. Structure–function relationship revealed that an olefinic conjugation bridge is critical in maintaining the charge-separated ground state.

The studies of the linear and nonlinear optical properties of **SZC** show moderate dipole moments and first hyperpolarizabilities. **SZC** can be doped up to 10% by weight into poly(ether sulfone) to form a uniform film. A chromophore-grafted polymer containing 14% by weight of **SZC** exhibits a promising EO coefficient (30 pm/V at 1550 nm). This versatile preparation method not only opens the new avenue for the design and synthesis of a variety of blue-shifted zwitterionic cyanopyridinium chromophores, but also enables easy further structure modification to achieve desired linear and nonlinear optical properties for specific applications.

Notes

The authors declare no competing financial interest.

Acknowledgments

We thank the Natural Sciences and Engineering Research Council of Canada and National Natural Science Foundation of China (21272061, 51272069) for financial support and Dr. W. Wenseleers of University Antwerp for measurement of the hyperpolarizability of **SZC** chromophores.

Appendix A. Supplementary data

Supplementary data related to this article can be found at http://dx.doi.org/10.1016/j.dyepig.2014.06.005.

References

[1] Bell NA, Crouch DJ, Simmonds DJ, Goeta AE, Gelbrich T, Hursthouse MB. Structural and solvatochromic studies of a series of tricyanoquinodimethane-based zwitterions. J Mater Chem 2002;12:1274–9.
[2] Marder SR, Gorman CB, Meyers F, Perry JW, Bourhill G, Bredas JL, et al. A unified description of linear and nonlinear polarization in organic polymethine dyes. Science 1994;265:632–5.
[3] Kay AJ, Woolhouse AD, Gainsford GJ, Haskell TG, Barnes TH, McKinnie IT, et al. A simple, novel method for the preparation of polymer-tetherable, zwitterionic merocyanine NLO-chromophores. J Mater Chem 2001;11:996–1002.
[4] Ashwell GJ. Photochromic and nonlinear optical properties of C16H33-P3CNQ and C16H33-Q3CNQ Langmuir-Blodgett films. Thin Solid Films 1990;186:155–65.
[5] Hao WH, McBride A, McBride S, Gao JP, Wang ZY. Colorimetric and near-infrared fluorescence turn-on molecular probe for direct and highly selective detection of cysteine in human plasma. J Mater Chem 2011;21:1040–8.
[6] Song N. Carleton University. [PhD thesis]; 2004.
[7] Szablewski M, Thomas PR, Thornton A, Bloor D, Cross GH, Cole JM, et al. Highly dipolar, optically nonlinear adducts of tetracyano-p-quinodimethane: synthesis, physical characterization, and theoretical aspects. J Am Chem Soc 1997;119:3144–54.
[8] Bai YW, Song NH, Gao JP, Sun X, Wang XM, Yu GM, et al. A new approach to highly electrooptically active materials using cross-linkable, hyperbranched chromophore-containing oligomers as a macromolecular dopant. J Am Chem Soc 2005;127:2060–1.
[9] Zeng Q, Li Z, Li Z, Ye C, Qin J, Tang B. Convenient attachment of highly polar azo chromophore moieties to disubstituted polyacetylene through polymer reactions by using "click" chemistry. Macromolecules 2007;40:5634–7.
[10] Dalton LR, Sullivan PA, Bale DH. Electric field poled organic electro-optic materials: state of the art and future prospects. Chem Rev 2010;110:25–55.
[11] Li ZA, Wu W, Li Q, Yu G, Xiao L, Liu Y, et al. High-generation second-order nonlinear optical (NLO) dendrimers: convenient synthesis by click chemistry and the increasing trend of NLO effects. Angew Chem Int Ed 2010;49:2763–7.
[12] Wu W, Wang C, Tang R, Fu Y, Ye C, Qin J, et al. Second-order nonlinear optical dendrimers containing different types of isolation groups: convenient synthesis through powerful "click chemistry" and large NLO effects. J Mater Chem C 2013;1:717–28.
[13] Luo J, Huang S, Shi Z, Polishak B, Zhou X, Jen AKY. Tailored organic electro-optic materials and their hybrid systems for device applications. Chem Mater 2011;23:544–53.
[14] Wu J, Peng C, Xiao H, Bo S, Qiu L, Zhen Z, et al. Donor modification of nonlinear optical chromophores: synthesis, characterization, and fine-tuning of chromophores' mobility and steric hindrance to achieve ultra large electro-optic coefficientsin guest-host electro-optic materials. Dyes Pigment 2014;104:15–23.
[15] Kang H, Facchetti A, Jiang H, Cariati E, Righetto S, Ugo R, et al. Ultralarge hyperpolarizability twisted π-electron system electro-optic chromophores: synthesis, solid-state and solution-phase structural characteristics, electronic structures, linear and nonlinear optical properties, and computational studies. J Am Chem Soc 2007;129:3267–86.
[16] Halter M, Liao Y, Plocinik RM, Coffey DC, Bhattacharjee S, Mazur U, et al. Molecular self-assembly of mixed high-beta zwitterionic and neutral ground-state NLO chromophores. Chem Mater 2008;20:1778–87.
[17] Liao Y, Bhattacharjee S, Firestone KA, Eichinger BE, Paranji R, Anderson CA, et al. Antiparallel-aligned neutral-ground-state and zwitterionic chromophores as a nonlinear optical material. J Am Chem Soc 2006;128:6847–53.
[18] Gao J, Cui Y, Yu J, Wang Z, Wang M, Qian G. Molecular design and synthesis of hetero-trichromophore for enhanced nonlinear optical activity. Macromolecules 2009;42:2198–203.
[19] Kay AJ, Woolhouse AD, Zhao Y, Clays K. Synthesis and linear/nonlinear optical properties of a new class of 'RHS' NLO chromophore. J Mater Chem 2004;14:1321–30.
[20] Metzger RM, Heimer NE, Aswell G. Crystal and molecular structure and properties of picolyltricyanoquinodimethan, the zwitterionic donor-π-acceptor adduct between Li^+ TCNQ- and 1,2-dimethylpyridinium iodide. Mol Cryst Liq Cryst 1984;107:133–49.
[21] Beaudin AMR, Song N, Men L, Gao JP, Wang ZY, Szablewski M, et al. Synthesis and properties of zwitterionic nonlinear optical chromophores with large hyperpolarizability for poled polymer applications. Chem Mater 2006;18:1079–84.
[22] Campo J, Wenseleers W, Goovaerts E, Szablewski M, Cross GH. Accurate determination and modeling of the dispersion of the first hyperpolarizability of an efficient zwitterionic nonlinear optical chromophore by tunable wavelength Hyper-Rayleigh scattering. J Phys Chem C 2008;112:287–96.
[23] Xiong Y, Tang H, Zhang J, Wang ZY, Campo J, Wenseleers W, et al. Functionalized picolinium quinodimethane chromophores for electro-optics: synthesis, aggregation behavior, and nonlinear optical properties. Chem Mater 2008;20:7465–73.
[24] Ibersiene F, Hammoutene D, Boucekkine A, Katan C, Blanchard-Desce M. DFT study of NLO properties of boroxine based octupolar molecules. J Mol Struct THEOCHEM 2008;866:58–62.
[25] Davies JA, Elangovan A, Sullivan PA, Olbricht BC, Bale DH, Ewy TR, et al. Rational enhancement of second-order nonlinearity: bis-(4-methoxyphenyl) hetero-aryl-amino donor-based chromophores: design, synthesis, and electrooptic activity. J Am Chem Soc 2008;130:10565–75.
[26] Blanchard-Desce M, Alain V, Bedworth PV, Marder SR, Fort A, Runser C, et al. Large quadratic hyperpolarizabilities with donor-acceptor polyenes exhibiting optimum bond length alternation: correlation between structure and hyperpolarizability. Chem Eur J 1997;3:1091–104.
[27] Andreu R, Blesa MJ, Carrasquer L, Garin J, Orduna J, Villacampa B, et al. Tuning first molecular hyperpolarizabilities through the use of proaromatic spacers. J Am Chem Soc 2005;127:8835–45.
[28] Olmsted J. Calorimetric determinations of absolute fluorescence quantum yields. J Phys Chem 1979;83:2581–4.
[29] Demas JN, Crosby GA. Measurement of photoluminescence quantum yields. J Phys Chem 1971;75:991–1024.
[30] Teng CC, Man HT. Simple reflection technique for measuring the electro-optic coefficient of poling polymers. Appl Phys Lett 1990;56:1734–6.
[31] Guseva TI, Senchenya NG, Golding IP, Mager KA, Gololobov YG. Synthesis of functionally substituted cyanoacetates. Russ Chem Bull 1993;42:478–80.
[32] Wu YL, Bures F, Jarowski PD, Schweizer WB, Boudon C, Gisselbrecht JP, et al. Proaromaticity: organic charge-transfer chromophores with small HOMO-LUMO gaps. Chem Eur J 2010;16:9592–605.
[33] Kawase T, Wakabayashi M, Takahashi C, Oda M. Dicyanodiaryl-p-quinodimethanes: an efficient synthesis using a new dilithium reagent and their solvent-dependent properties. Chem Lett 1997;1055–1056.
[34] Hao WH, Wang C, Qian G, Wang ZY. (Z)-1,1-Dicyano-2-(4-fluorophenyl)-3-(1-hexylpyridin-1-ium-4-yl)prop-2-en-1-ide. Acta Cryst 2012;E68:o82.
[35] Allen FH, Kennard O, Watson DG, Brammer L, Orpen AG, Taylor R. Tables of bond lengths determined by x-ray and neutron diffraction. Part 1. Bond lengths in organic compounds. J Chem Soc Perkin Trans 1987;2:S1–19.
[36] De Ridder DJA, Heijdenrijk D, Schenk H, Dommisse RA, Lemiere GL, Lepoivre JA. Structure of 4-{2-[1-methyl-4(1H)-pyridylidene]ethylidene} cyclohexa-2,5-dien-1-one trihydrate. Acta Crystallogr 1990;C46:2197–9.
[37] Wurthner F, Yao S, Debaerdemaeker T, Wortmann R. Dimerization of merocyanine dyes. Structural and energetic characterization of dipolar dye

aggregates and implications for nonlinear optical materials. J Am Chem Soc 2002;124:9431–47.
[38] Reichardt C. Solvatochromic dyes as solvent polarity indicator. Chem Rev 1994;94:2319–58.
[39] Lide DR. Handbook of chemistry and physics. 76th ed. Boca Raton: CRC Press Inc.; 1995–1996P8–64.
[40] Benson RC, Kues HA. Absorption and fluorescence properties of cyanine dyes. J Chem Eng Data 1977;22:379–83.
[41] Katz HE, Singer KD, Sohn JE, Dirk CW, King LA, Gordon HM. Greatly enhanced second-order nonlinear optical susceptibilities in donor-acceptor organic molecules. J Am Chem Soc 1987;109:6561–3.
[42] Shi Y, Zhang C, Zhang H, Bechtel H, Dalton LR, Robinson BH. Low (sub-1-volt) halfwave voltage polymeric electro-optic modulators achieved by controlling chromophore shape. Science 2000;288:119–22.
[43] Song N, Men L, Gao JP, Bai YW, Beaudin AMR, Yu GM, et al. Cross-linkable zwitterionic polyimides with high electro-optic coefficients at telecommunication wavelengths. Chem Mater 2004;16:3708–13.
[44] Macchi R, Cariati E, Marinotto D, Roberto D, Tordin E, Ugo R, et al. Stable SHG from in situ grown oriented nanocrystals of [(E)-N,N-dimethylamino-N′-methylstilbazolium][p-toluenesulfonate] in a PMMA film. J Mater Chem 2010;20:1885–90.